J Nanopart Res (2016) 18:155
DOI 10.1007/s11051-016-3468-0

RESEARCH PAPER

Reliable and well-controlled synthesis of noble metal nanoparticles by continuous wave laser ablation in different liquids for deposition of thin films with variable optical properties

S. M. Arakelyan · V. P. Veiko · S. V. Kutrovskaya · A. O. Kucherik · A. V. Osipov · T. A. Vartanyan · T. E. Itina

Received: 31 December 2015 / Accepted: 30 May 2016 / Published online: 9 June 2016

Abstract We report the results of continuous wave laser interactions with both gold and silver targets in the presence of different liquids (deionized water, ethanol, and glycerol). Upon moderate laser irradiation at wavelength of 1.06 nm during 30 min, nanoparticle colloids are shown to be formed with surprisingly narrow size distributions and average dispersion as small as 15–20 nm. The average particle sizes range between 8 and 52 nm for gold and between 20 and 107 nm for silver. This parameter is shown to be stable and well-controlled by such laser parameters as intensity and effective irradiation time, as well as by the choice of the liquid phase. The possibilities of an efficient control over the proposed synthesis techniques are discussed, and the results of a bimetallic Au–Ag structure deposition from the obtained colloids are presented. The formation of the extended arrays of gold and silver nanoparticles with controlled morphology is examined. The changes in the optical properties of the obtained thin films are found to depend on their morphology, in particular, on the particle size, and distance between them.

Keywords Continuous laser · Colloidal solution · Nanoparticles · Processing

S. M. Arakelyan · S. V. Kutrovskaya · A. O. Kucherik · A. V. Osipov
A.G. and N.G. Stoletov Vladimir State University (VSU), 87 Gorki St., 600000 Vladimir, Russia
e-mail: arak@vlsu.ru

S. V. Kutrovskaya
e-mail: 11stella@mail.ru

A. O. Kucherik
e-mail: kucherik@vlsu.ru

A. V. Osipov
e-mail: osipov@vlsu.ru

V. P. Veiko · T. A. Vartanyan
St. Petersburg National Research University of Information Technologies, Mechanics and Optics, St. Petersburg 197101, Russia
e-mail: vadim.veiko@mail.ru

T. A. Vartanyan
e-mail: tvartanyan@corp.ifmo.ru

T. E. Itina (✉)
Laboratoire Hubert Curien, Université de Lyon, UJM-Saint-Etienne, CNRS, UMR5516, 42023 Saint-Etienne, France
e-mail: tatiana.itina@univ-st-etienne.fr

Introduction

Nanoparticles of noble metals are widely used for various applications in many areas such as nanophotonics, nano- and microelectronics, and photochemistry. The development of these applications relies on the properties of the generated structures that start deviating from those of massive samples when the particle size drops below around 100 nm (Lee and El-Sayed 2006; Letfullin et al. 2006; Mafune et al. 2003; Sylvestre et al. 2004). Such dimensional effects change characteristic parameters of various processes (the frequency of plasmon resonance, electron free path length and others) and define physicochemical properties of nanosystems.

Thin-nanostructured noble-metallic films demonstrate nonlinear optical effects in visible spectral range because of their plasmonic properties (Genov et al. 2004). In addition, optical characteristics of these thin films strongly depend on the period of the formed surface structures (Destouches et al. 2014). If the distance between the deposited particles is close to their sizes, the optical properties of the randomly deposited structures may considerably differ from these of periodical structures (Persson and Liebsch 1983). Thus, sintering of the bimetallic gold and silver complexes results in pronounced changes of the optical properties (Sonay et al. 2012). In this case, both morphology and shape of the deposited particles influence the final optical properties. One of the challenging issues in the demonstration of the scale-effect for metallic thin films is the control over particles size.

Laser ablation is considered to be one of the versatile methods of nanoparticle generation that allows a reliable control over particle sizes (Sylvestre et al. 2004). In particular, the presence of nanoparticles was demonstrated in pulsed laser deposition performed both in vacuum and in inert gases (Gouriet et al. 2009). Laser ablation in liquid media, furthermore, was shown to be a promising approach for a wide range of applications (Abramov et al. 2014; Barmina et al. 2010; Itina 2011; Simakin et al. 2001). In contrast to nanoparticles synthesized by chemical techniques, nanoparticles generated by laser ablation in liquids can be free of surface active substances and irrelevant ions (Barcikowski et al. 2007), thus providing a possibility of generating chemical "pure" colloids.

The properties of nanoparticles generated by laser ablation in liquids depend on many parameters, such as laser wavelength, laser pulse duration, laser fluence, material absorption, and choice of the liquid. (Barcikowski et al. 2007; Barmina et al. 2010; Besner et al. 2007; Riabinina et al. 2012). One of the main difficulties in the application of high-intensity laser sources is high plasma energy and droplet formation, which are really hard to avoid. When pulsed lasers are used, furthermore, laser intensity is typically sufficiently high for laser-induced nanoparticle fragmentation to occur during nanoparticle formation in colloids, considerably complicating the prediction of the experimental results. In fact, strong shock waves, phase transitions, and cavitation bubbles are known to be generated by both nanosecond and femtosecond pulse durations. Under such conditions, not only target is affected by laser action, but also particles, if they are present in the surrounding liquid (Akman et al. 2011; Lee and El-Sayed 2006). In addition, such effects as optical breakdown and liquid decomposition were reported to occur at high laser intensities (Liu et al. 2009). These effects can result in uncontrollable changes in both particle size and size distribution.

When a continuous wave laser is used for nanoparticle production, and its intensity is typically orders of magnitude smaller than the one in pulse-periodic regime. The role of laser is mostly thermal in this case. For a particular range of laser intensities, melting of the target is expected leading to a molten bath/layer formation, whose thickness is defined by the coefficient of thermal diffusion of the target material. However, liquid is typically heated too, and its convective movement can prevent the formation of shock waves, of a cavitation bubble, or of a gas cavity with a high gas pressure. Therefore, both the mechanisms and sizes of nanoparticle formed by continuous wave laser are different from the ones in pulsed-periodic regime and are not yet completely understood.

Here, we present an experimental study of the interaction of a continuous laser radiation with noble metal targets in liquid media. We show that such a choice of the laser system can provide a possibility of a reliable control over mean nanoparticle dimensions and over the dispersion. The obtained results are analyzed as a function of laser parameters for several liquids (deionized water, ethanol, and glycerol), and the involved mechanisms are then discussed.

Furthermore, we present the results of laser-induced thermal deposition of nanoparticles from the colloids leading to the formation of bimetallic clusters on a transparent substrate. The possibility of a bimetallic multilayer formation with controllable morphology is demonstrated. Optical properties and possible applications of the obtained structures are finally discussed.

Synthesis of nanoparticles by CW laser irradiation in liquids

Experimental details

The process of noble metal nanoparticle formation is examined under continuous wave (CW) laser scanning of bulk metal targets composed of 99.9 % Au or of 99.9 % Ag placed in a liquid medium. In the presented experiments, Ytterbium fiber (Yb-fiber) laser with a diode pumping was used. A laser beam with the diameter $d = 30 \div 100$ μm was focused on the target surface proving the radiation intensity from 10^5 to 10^6 W/cm^2. Laser scanning was performed by varying the motion speed v of a mechanized table between 1 μm/s and 1 mm/s with a minimum step of 1 μm. Thus, the characteristic time of laser action $\tau = d/v$ could be varied from 0.01 to 10 s by changing either d or v. The total laser scanning time was 30 min within around 1 mm length at the surface.

Laser power was varied in the range from 40 to 100 W. The following liquids were used as a solvent: ethanol (C_2H_5OH), glycerol ($C_3H_5(OH)_3$), and deionized water (H_2O). Thus, we varied such parameters as liquid viscosity, compressibility, heat conductivity, boiling, and evaporation temperatures. These liquid properties are known to determine the expected thermodynamic and hydrodynamic effects when nanoparticles are produced in liquid colloids (Abramov et al. 2014; Linz et al. 2015). However, their roles are not yet completely understood. In what follows, we analyze the corresponding effects produced using either CW or nanosecond laser.

Experimental results

CW laser-induced particle formation and their sizes

Figure 1 demonstrates the central part of the target surface after the action of a continuous laser radiation with beam diameter of 100 μm and surface scanning velocity of 100 μm/s. Laser power was varied from 40 to 100 W. With the increase in laser power, the evidences of local melting of the thin layer in the central part of laser-irradiated area becomes more and more pronounced (Fig. 1c–d). For the largest used laser power, a channel with depth up to 5 μm was formed on both gold and silver target surfaces. This depth was determined during the cavity structure examination and the sample was bent by 20 °C with respect to the normal. Similar procedure was used for both gold and silver, and the difference in depth was negligible in the considered laser intensity range.

As a result of laser irradiation of silver target, similar structures are found to be formed at the surface (Fig. 2). Because thermal conductivity of silver is smaller than that of gold, thermal effects are more pronounces here, and the resulting surface structures are larger.

After laser irradiation, the sizes of the particles were measured in the colloid using the particle dimension analyzer based on the principle of the dynamic light diffusion (Horiba LB-550). The corresponding size distributions are shown in Fig. 3. The values presented in Figure are averaged by six consecutive measurements, where the time difference between the measurements is one minute. We note that no considerable change in time was observed. These results prove high colloidal stability, which is confirmed by measuring zeta-potential of the obtained colloid systems in the range of 18–35 mV during 30 days with the increase in laser radiation intensity. In addition to the confirmed stability, these results demonstrate that the obtained distributions are surprisingly narrow, with size dispersion on the order of the mean size. Interestingly, neither bimodal size distribution nor distribution with a long tail was obtained.

Now, when relatively small particle size, good stability, and dispersion are confirmed, we turn to the role of both laser parameters and material/liquid properties. First, we vary laser parameters, such as laser intensity and the mean irradiation time.

Figure 4 clearly demonstrates the effect of laser intensity on the mean nanoparticle sizes. One can see experimentally measured mean nanoparticle diameter for both gold and silver targets placed in different liquids.

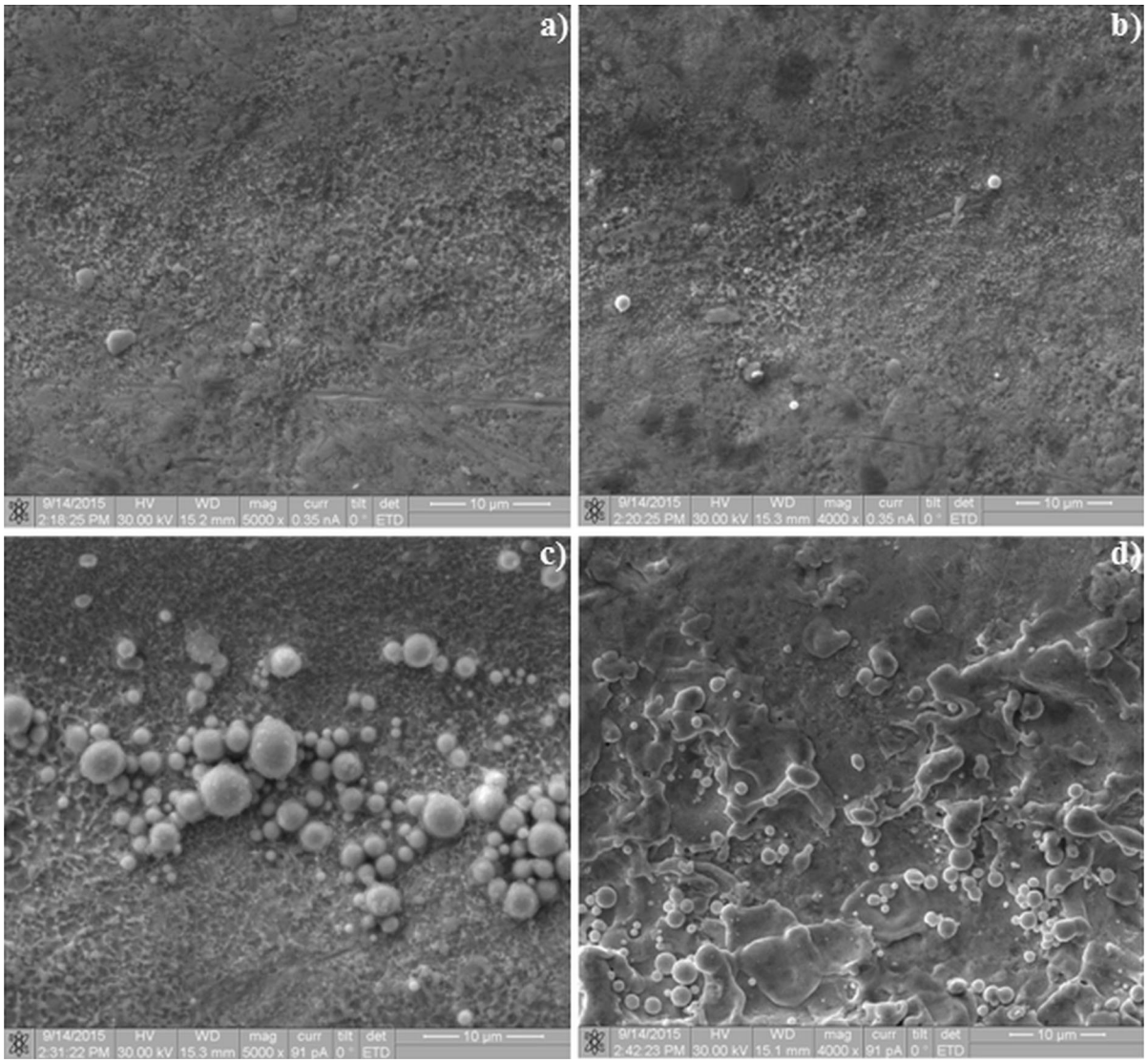

Fig. 1 Scanning electric microscope (SEM) images of Au target after continuous laser irradiation with beam diameter of 100 μm and laser power of **a** 40 W, **b** 60 W, **c** 80 W, and **d** 100 W. All images present the central part of the laser-irradiated area

In addition, the mean particle diameters and the mean dispersion are summarized in Table 1. We note that because the distributions are not symmetric, the mean diameters provide just an indication of particle sizes, and particle size dispersion varies with change in liquid. Interestingly, the dispersion is smaller in glycerol and increases when water and ethanol are used.

When a CW laser is used, another important parameter is typically laser irradiation time. Figure 5 shows how this parameter affects sizes of laser-generated particles. Here, silver target was irradiated with laser beams of different intensities. One can clearly see that the particle diameter can be also controlled by the laser irradiation time. In particular, a considerable growth is observed when the laser irradiation time rises from 5 and 10 s. However, it is still possible to obtain smaller nanoparticles with diameters of 20–40 nm by choosing higher scanning speed.

The obtained results can be explained by the peculiarities of the nanoparticle formation processes

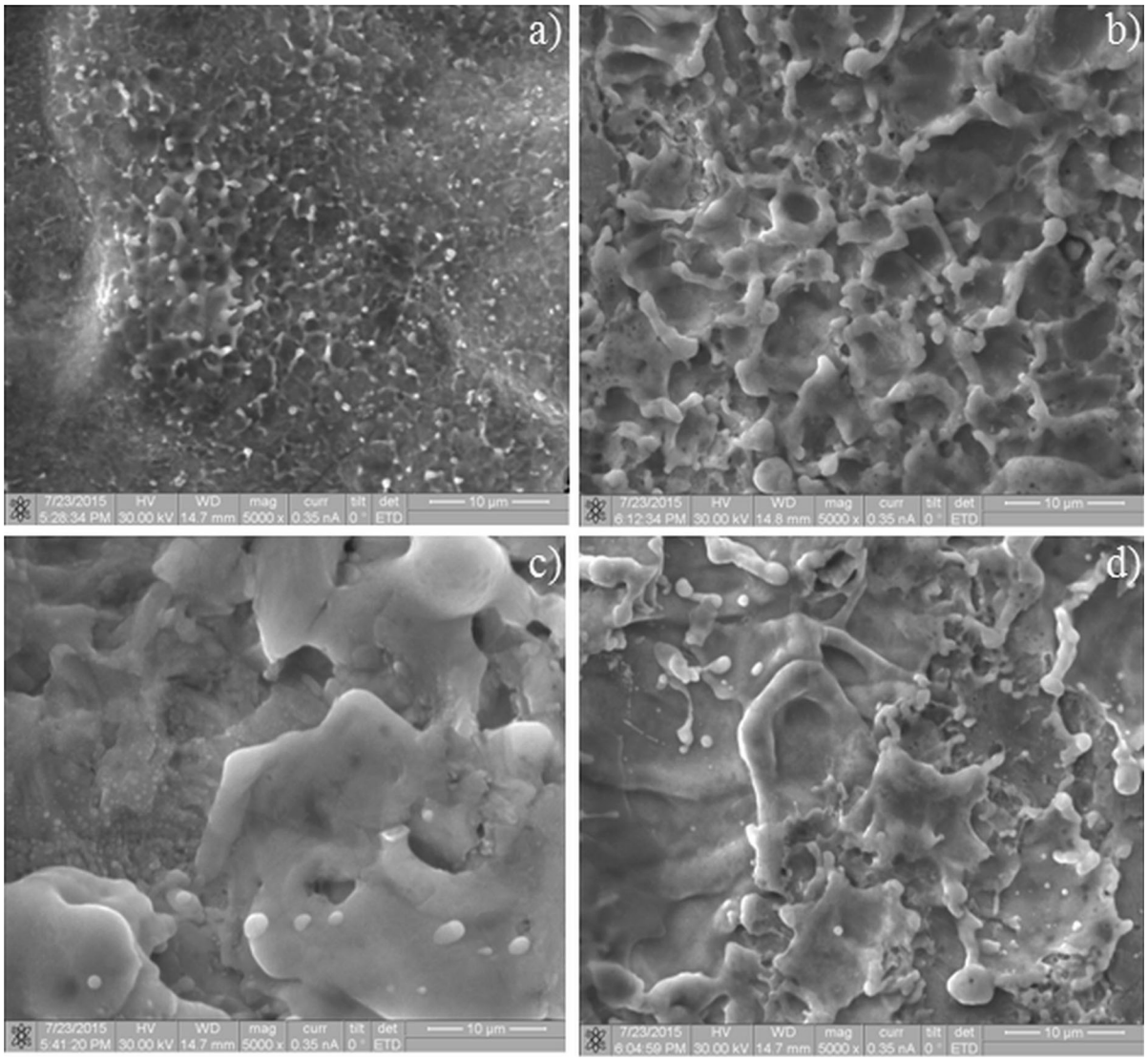

Fig. 2 SEM images of the silver target after continuous laser irradiation with beam diameter of 100 μm and laser power of **a** 40 W, **b** 60 W, **c** 80 W, and **d** 100 W. All the images show the central part of the laser-irradiated area

by the CW laser in liquids. Typically, CW laser irradiation leads to both liquid and metal heating followed by metal material ejection and nanoparticle formation. The more material is ejected from the target, the larger is the primary nanoparticle diameter. Evidently, a raise in laser intensity and/or in the effective laser irradiation time increases temperatures of both the metal target and of the surrounding liquid. Even if the ambient liquid does not absorb laser radiation, a part of energy is transferred from the heated metal to the surrounding medium, leading to such effects as nanobubbles formation near the metal surface, absorbing plasma layer, or to liquid boiling at higher laser intensities. Nanobubble collapse gives rise to the metal surface erosion and to the following nucleation of small metallic nanoparticles. If, furthermore, metal melting point is reached, the melted layer gets thicker with both laser intensity and laser irradiation time. This layer suffers not only from the recoil pressure, but also

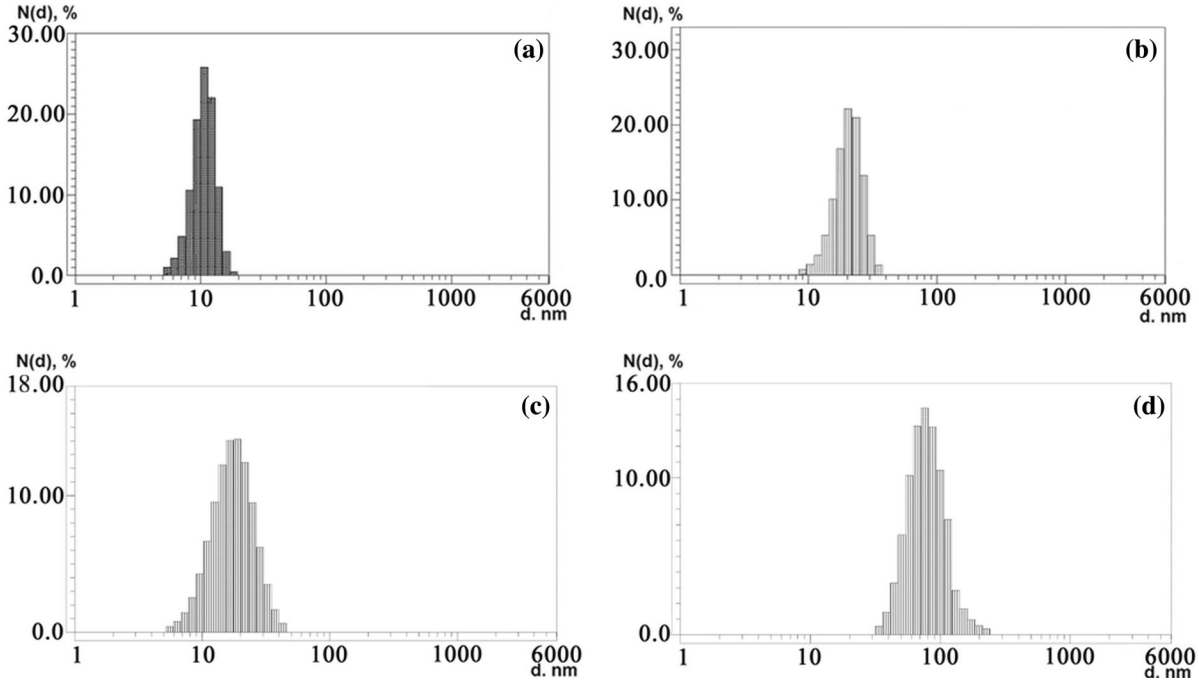

Fig. 3 Size distribution histograms obtained for **a** gold and **b** silver after continuous laser irradiation in glycerol with laser intensity $I = 10^5$ W/cm^2. Similar results obtained for **c** gold and **d** silver with $I = 10^6$ W/cm^2

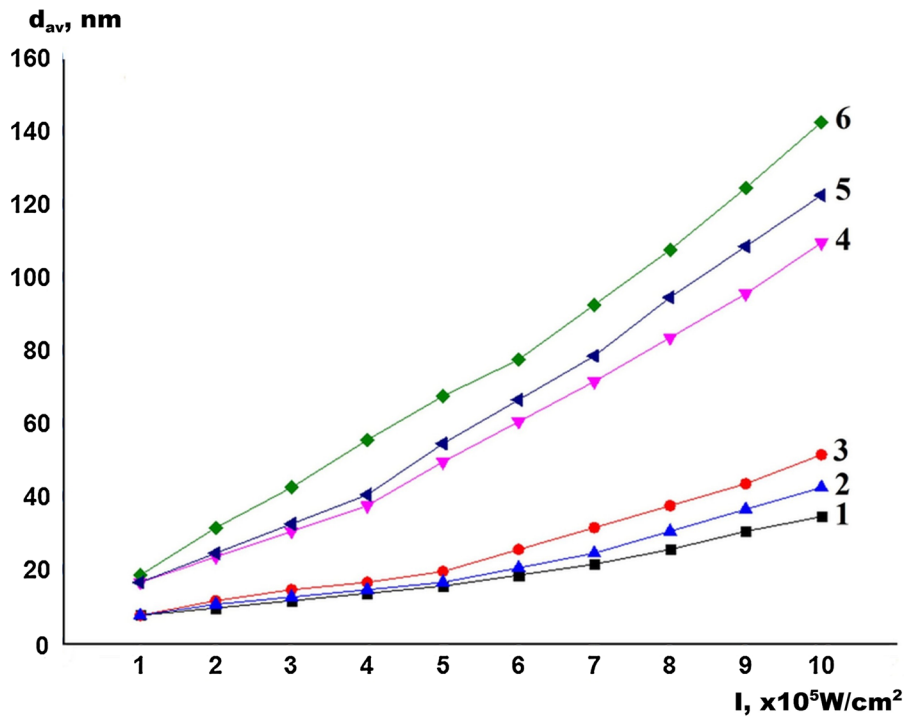

Fig. 4 The average size, d_{av}, of the generated gold and silver nanoparticles as a function of laser intensity for different liquids: *1* gold in glycerol; *2* gold in water; *3* gold in ethanol; *4* silver in glycerol; *5* silver in water; and *6* silver in ethanol. Here, laser scanning velocity is 100 μm/s

Table 1 Nanoparticle diameter range obtained in the presented experiments

No.	Laser action parameters (intensity I, time of action t)	Liquid phase	Target	Average diameter of synthesized particles, nm
1	$I = 10^5$–10^6 W/cm^2 $t = 30$ min	$C_3H_5(OH)_3$	Au	8–34
		C_2H_5OH		10–52
		H_2O		8–38
		$C_3H_5(OH)_3$	Ag	21–88
		C_2H_5OH		37–125
		H_2O		29–107

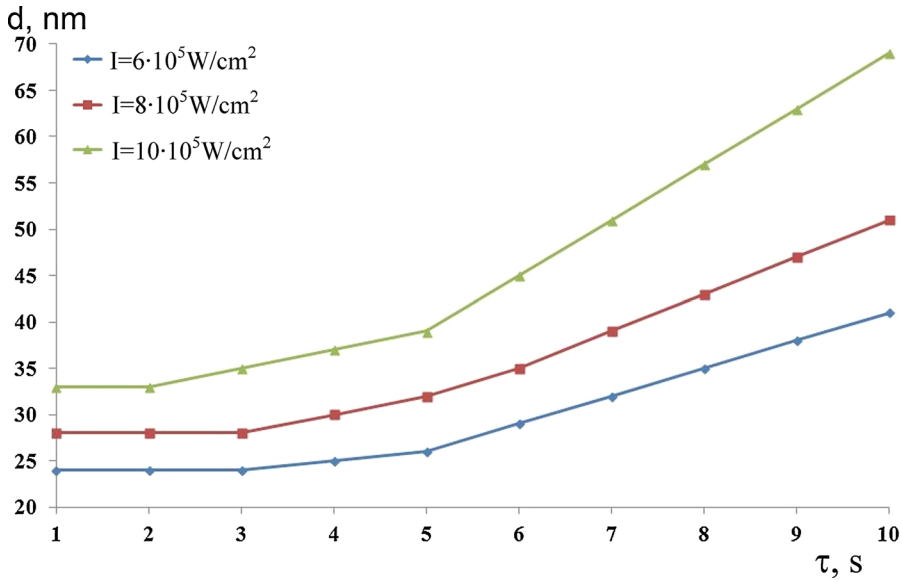

Fig. 5 Silver nanoparticle sizes obtained in deionized water as a function of effective laser action time τ for several laser intensities. Here, laser spot size is 100 μm, laser scanning velocity is 10–100 μm/s, and the total scanning time is 30 min

from the instabilities that commonly arise due to strong temperature gradients resulting in nanoparticle formation too (Herminghaus et al. 1998). We note that nanoparticle aggregation is prevented in this regime because of the liquid convection flow that continuously removes particles from the laser-affected zone during laser irradiation. The convection flow takes place due to the strong temperature gradients and depends both on liquid properties and on laser parameters (Gatskevich et al. 1995). Aggregation becomes, however, possible after the end of laser irradiation. Colloid density is, however, not high enough at this time. More detailed study of the proposed mechanisms is underway and will be presented elsewhere.

Nanoparticle morphology and optical properties

To examine the particles shape and structure, we used the transmission electronic microscope (TEM). The obtained results are presented in Fig. 6. These images demonstrate that mostly spherical and crystal particles are generated. The crystal structure analysis provided a characteristic period of gold nanoparticle lattice, d, of 2.35 ± 0.05 angstroms for (111)Au interplanar spacing, whereas d = 2.06 ± 0.05 Å for (002)Au.

The lattice constant of silver particles is found to be d = 2.36 ± 0.04 Å for (111)Ag interplanar spacing. In addition, one can see Debye rings in the diffraction picture obtained for the direction of an X-ray beam parallel to the (100) surface. We note that these rings

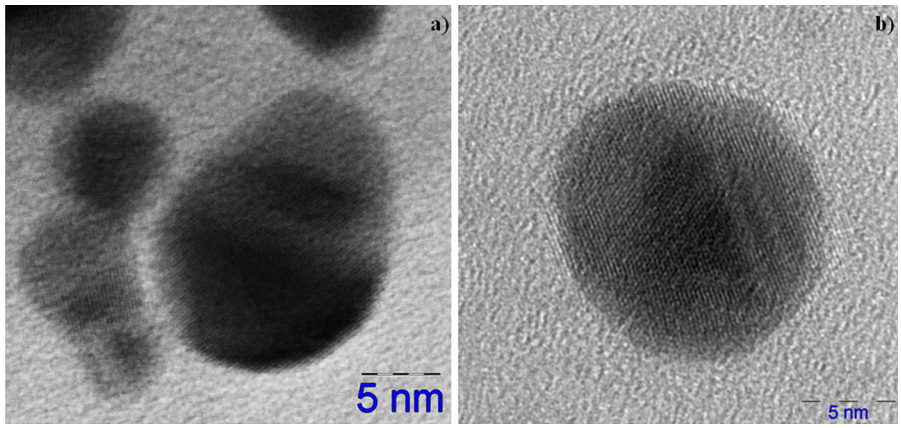

Fig. 6 TEM images of **a** gold and **b** silver nanoparticles generated in water. Here, laser intensity is 2×10^5 W/cm^2, and the total laser scanning time is 30 min

are typical to polycrystal structures with very small sizes of crystals and correspond to fcc lattice.

The performed TEM analysis indicates that the obtained nanoparticles are mainly affected by the processes of their self-assembly in the colloid after laser ablation. In principle, particles can be also heated by a rather weak laser energy absorption, or by the heat exchange with the surrounding liquid. These effects commonly lead to particle reshaping or even fragmentation (Antipov et al. 2012; Makarov 2013). This process can become particularly important if liquid is heated up to a supercritical state (Abramov et al. 2014).

To check if laser radiation affects nanoparticle formation, the generated colloidal solutions were irradiated again under the conditions, which are similar to the process of their synthesis at the wavelength of 1064 nm, but without metal target. The cell with colloid was moved with a speed of 10 mkm/s. The laser beam was focused, so that the focal spot diameter was $\sim$50 μm. The focal position was fixed in the colloidal volume at the height of 1 mm from the cell bottom. No liquid boiling was noticed during laser action. In fact, liquid temperature increased only by $\sim$20 °C in the presented experiments. Interestingly, a repeated irradiation of colloids does not result in the particle size decay, neither in the change of the particle shape (Fig. 7).

Figure 7 shows that the particles maintained their crystal structure, but a major part of them gathered into agglomerates. In addition, particles of a smaller size and irregular shape were attached to larger spherical particles in most cases.

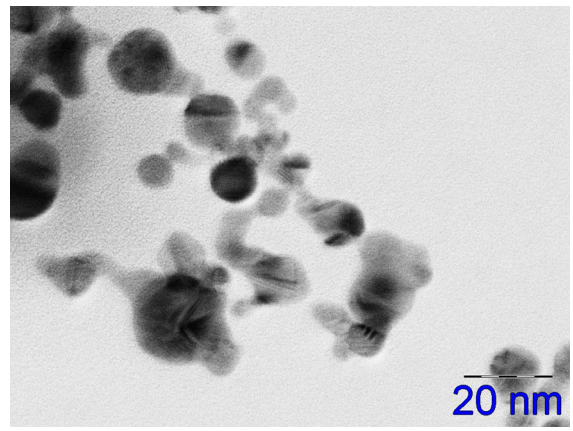

Fig. 7 Gold nanoparticles generated during the second irradiation of the generated colloid by the continuous laser radiation with laser wavelength of 1064 nm at laser intensity of 10^6 W/cm^2. Here, the total laser scanning time is 30 min

The measured optical parameters of the obtained colloidal systems are shown in Fig. 8. The spectra were measured by the spectrophotometer SF-2000. Interestingly, similar optical properties are observed for each metal in various liquids. Only small shifts in the absorption maxima corresponding to the plasmon resonance of silver ($\sim$390 nm) and gold ($\sim$520 nm) are observed.

In fact, the measured absorption spectra indicate that silver oxide was not produced in the process of laser irradiation of the system. We also note that the

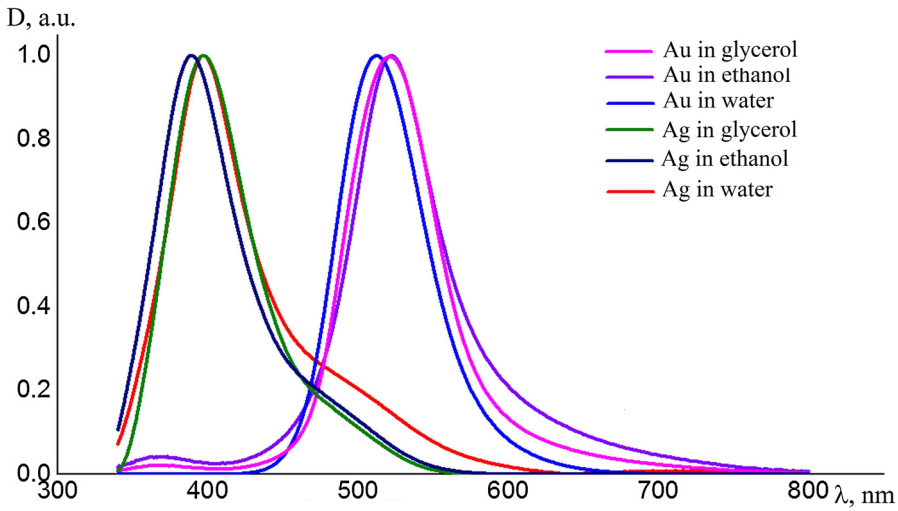

Fig. 8 Normalized optical absorption coefficient spectra of nanoparticle colloids formed by continuous laser irradiation of silver and gold targets located in different liquid phases. Here, the following laser parameters ARE used: laser power is 2×10^5 W/cm^2; mean laser irradiation time is 1 s, and laser spot size is 100 μm

obtained colloidal systems are stable. Thus, the observed changes in the spectrum were observed only 7–12 days after the laser irradiation, whereas a precipitation was observed at a delay of more than a month.

Bimetallic Au–Ag structure deposition and their optical properties

For the deposition of the bimetallic structures, the colloidal systems of both metals were mixed in equal proportions. The glass substrate was placed in the mixed solution. The deposition of thin film was made by laser irradiation as described by Antipov et al. (2012). Here, we used Yb-fiber laser ($\lambda = 1.06$ μm) with pulse duration of 100 ns and with laser repetition rate of 20 kHz. The average power was from 1.5 W up to 4.5 W, and the diameter of the laser beam was around 5 μm. The array of nanoparticles was formed on the substrate surface by repeated (up to 10 times) laser beam scanning along one and the same direction. The scanning speed was varied from 0.6 mm/s up to 1.5 mm/s. The length of the obtained array of nanoparticles was ~100 μm, whereas the average transverse dimension was ~5 μm, and the average height was about 55 nm.

The morphological and chemical composition of the deposited structures was studied by the scanning electron microscope Quanta 200 3D (Fig. 9) and using the atomic force microscope Ntegra-Aura (Fig. 10).

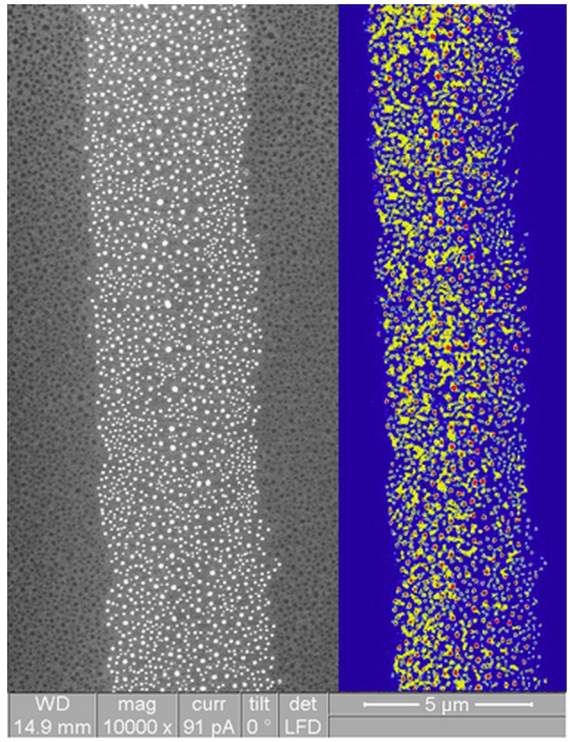

Fig. 9 Images obtained after deposition of bimetallic array of nanoparticles/clusters (size of initial particles about 50 nm) on the surface of pyrolytic graphite. Both Quanta 200 3D results and X-ray elemental analysis (EDAX) are shown. *Red markers* correspond to gold, whereas *yellow ones* correspond to silver. (Color figure online)

Figure 10 clearly demonstrates the formation of a quasi-ordered array of nanoparticles/clusters. By changing the initial size of particles in the colloid,

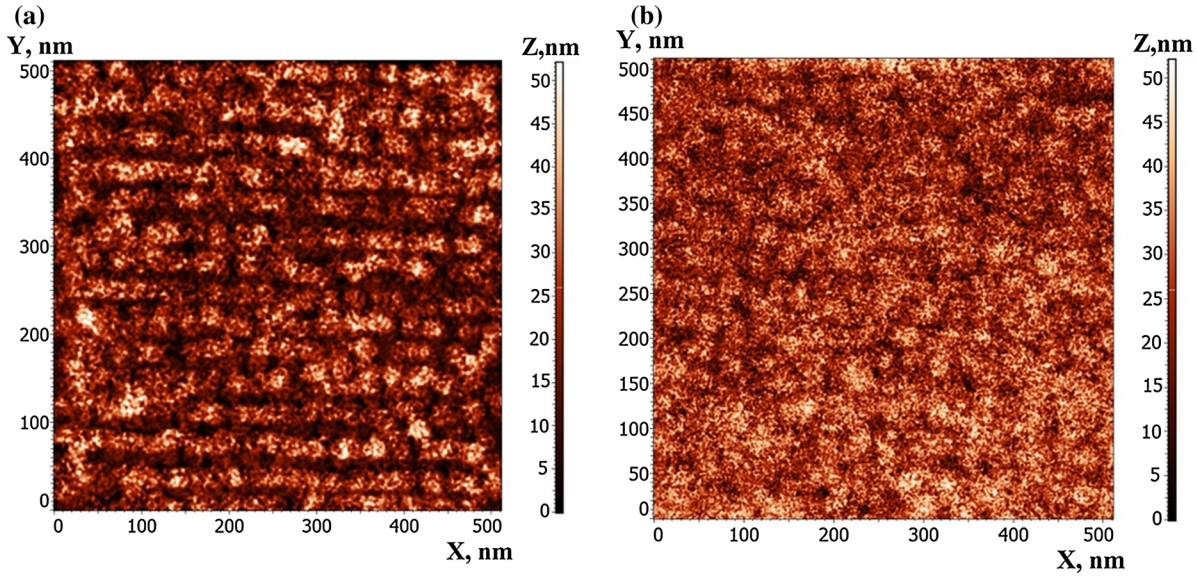

Fig. 10 AFM images of deposited thin films Au–Ag from colloidal system on the surface of a glass substrate KB8. Here, concentration was about 1 μg/ml. The initial particle sizes were 50 nm (**a**) and 10 nm (**b**). The average height of the relief on *left* image is 50 nm, whereas it is 48 nm on the *right*. The average distance between particles is 5 nm in (**a**) and 2 nm in (**b**). The sizes and distances between particles were studied by Grain Analysis library, which is included in the Image Analysis tool (NT-MDT)

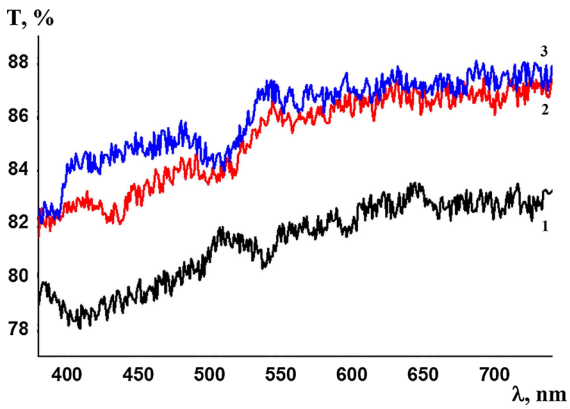

Fig. 11 Measured transmission spectra of deposited Au:Ag layers: *1* Au:Ag (1:1), the particle diameter is about 50 nm, one layer, the distance between particles is about 5 nm; *2* Au:Ag (1:1), the particle diameter is about 10 nm, five layers, the distance between particles is about 4 nm; *3* Au:Ag (1:1), the particle diameter is about 10 nm, five layers, the distance between particles is about 2 nm

the morphology of the deposited layer was modified. Changing laser irradiation parameters, such as the average power and the scanning speed, one can efficiently to control over the deposition process. This method allows us to correlate the optical properties of thin bimetallic films with other properties, such as the initial particle sizes, the number of layers, and the distance between the particles.

Finally, optical properties of the deposited thin films were studied in the visible part of spectrum using spectrophotometer SF-2000 (Fig. 11). It was found that the all the produced film spectra are rather complex, but lie in the visible range. The broad absorption band between 360 and 420 nm may be ascribed to the localized surface plasmon in silver nanoparticles. However, changes in particle parameters and, particularly, their distribution on the substrate could result in the considerable spectral changes. For example, the transmission of the layer increases in the case of 50 nm particles in the spectral range of the localized surface plasmon of gold nanoparticles (from 520 to 560 nm). This value, however, drops down in the case of 10 nm particles. Interestingly, the transmission of the 5-layer system of 10 nm particles is higher than that of one-layer system of 50 nm particles.

Conclusion

In this paper, we have presented the experimental results obtained in laser ablation of massive targets

made of gold and silver in the presence of a liquid. A possibility of an efficient control over nanoparticle generation is demonstrated. In fact, both the required size and size distribution have been found to depend on the laser parameters and the choice of the liquid component. In contrast to the cases of intense pulsed-periodic laser interactions with short- and ultra-short pulse duration, in the considered case of a gentle CW laser irradiation, it is possible to avoid many uncontrollable processes occurring during nanoparticle formation, such as shock wave propagation, optical breakdown, particle aggregation, and chemical decomposition.

In addition, laser-induced thermal deposition of nanoparticles from the colloids has been shown to result in the formation of bimetallic clusters on a transparent substrate. The obtained results have demonstrated the influence of morphology (particle diameter in the colloid, the distance between the deposited particles, the number of layers, etc.) on the optical properties of the deposited thin film of bimetallic clusters. The optical properties of the deposited bimetallic films are shown to change as a function of their material and structural parameters in a highly predictable way.

The reported well-controlled formation of colloidal nanoparticles and their deposition are of a great interest for further development of thin films and cluster-based elements of photonics, such as periodic structures/photon crystals, gradient materials, as well as films with the required optical properties.

Acknowledgments The study was supported by the Ministry of Education and Science of the Russian Federation (state project no. 2014/13), RBFR Grant number 16-32-60067 mol_a_dk, by the Government of Russian Federation (Grant no. 074-U01), and by France-Russia collaborative project PICS 6106 of DRI CNRS, France.

References

Abramov DV, Antipov AA, Arakelian SM, Khor'kov KS, Kucherik AO, Kutrovskaya SV, Prokoshev VG (2014) New advantages and challenges for laser-induced nanostructured cluster materials: functional capability for experimental verification of macroscopic quantum phenomena. Laser Phys. 24:074010. doi:10.1088/1054-660X/24/7/074010

Akman E, Genc Oztoprak B, Gunes M, Kacar E, Demir A (2011) Effect of femtosecond Ti:Sapphire laser wavelengths on plasmonic behaviour and size evolution of silver nanoparticles. Photon Nanostruct Fundam Appl 9:276–286. doi:10.1016/j.photonics.2011.05.004

Antipov AA, Arakelyan SM, Kutrovskaya SV, Kucherik AO, Makarov AA, Nogtev DS, Prokoshev VG (2012) Pulse laser deposition of cluster nanostructures from colloidal single-component systems. Bull Russian Acad Sci Phys 76:611–617. doi:10.3103/S106287381206007X

Barcikowski S, Menéndez-Manjón A, Chichkov B, Brikas M, Raiukaitis G (2007) Generation of nanoparticle colloids by picosecond and femtosecond laser ablations in liquid flow. Appl Phys Lett 91:083113. doi:10.1063/1.2773937

Barmina EV, Stratakis E, Fotakis K, Shafeev GA (2010) Generation of nanostructures on metals by laser ablation in liquids: new results. Quantum Electron 40:1012–1020. doi:10.1070/QE2010v040n11ABEH014444

Besner S, Kabashin AV, Meunier M (2007) Two-step femtosecond laser ablation-based method for the synthesis of stable and ultra-pure gold nanoparticles in water Appl. Phys A 88:269–272. doi:10.1007/s00339-007-4001-1

Destouches N, Crespo-Monteiro N, Vitrant G, Lefkir Y, Reynaud S, Epicier T, Liu Y, Vocanson F, Pigeon F (2014) Self-organized growth of metallic nanoparticles in a thin film under homogeneous and continuous-wave light excitation. J Mater Chem C 2:6256–6263. doi:10.1039/C4TC00971A

Gatskevich EI, Ivlev GD, Chaplanov AM (1995) Melting and solidification of the surface layer of single-crystal silicon heated by pulsed laser radiation. Quantum Electron 22:801–806. doi:10.1070/QE1995v025n08ABEH000466

Genov DA, Sarychev AK, Shalaev VM, Wei A (2004) Resonant field enhancements from metal nanoparticle arrays. Nano Lett 4:153–158. doi:10.1021/nl0343710

Gouriet K, Sentis M, Itina TE (2009) Molecular dynamics study of nanoparticle evaporation and condensation in a gas. J Phys Chem C 113:18462–18467. doi:10.1021/jp9046648

Herminghaus S, Jacobs K, Mecke K, Bischof J, Fery A, Ibn-Elhaj M, Schlagowski S (1998) Spinodal dewetting in liquid crystal and liquid metal films. Science 282:916–919. doi:10.1126/science.282.5390.916

Itina TE (2011) On nanoparticle formation by laser ablation in liquids. J Phys Chem C 115:5044–5048

Lee K, El-Sayed M (2006) Gold and silver nanoparticles in sensing and imaging: sensitivity of plasmon response to size, shape, and metal composition. J Phys Chem B 110:19220–19225. doi:10.1021/jp062536y

Letfullin R, Joenathan C, George T, Zharov V (2006) Laser-induced explosion of gold nanoparticles: potential role for nanophotothermolysis of cancer. Nanomedicine 1:473–480. doi:10.2217/17435889.1.4.473

Linz N, Freidank S, Liang X-X, Vogelmann H, Trickl T, Vogel A (2015) Wavelength dependence of nanosecond infrared laser-induced breakdown in water: evidence for multi-photon initiation via an intermediate state. Phys Rev B 91:134114. doi:10.1103/PhysRevB.91.134114

Liu Z, Yuan Y, Khan S, Abdolvand A, Whitehead D, Schmid M, Li L (2009) Generation of metal-oxide nanoparticles using continuous-wave fibre laser ablation in liquid. J Micromech Microeng 19:054008. doi:10.1088/0960-1317/19/5/054008

Mafune F, Kohno J, Takeda Y, Kondow T (2003) Formation of stable platinum nanoparticles by laser ablation in water. J Phys Chem B 107:4218–4223. doi:10.1021/jp021580k

Makarov GN (2013) Laser applications in nanotechnology: nanofabrication using laser ablation and laser nanolithography. Phys Usp 56:643–682. doi:10.3367/UFNe.0183.201307a.0673

Persson BNJ, Liebsch A (1983) Optical properties of two-dimensional systems of randomly distributed particles. Phys Rev B 28:4247–4254. doi:10.1103/PhysRevB.28.4247

Riabinina D, Chaker M, Margot J (2012) Dependence of gold nanoparticles production on pulse duration by laser ablation in liquid media. Nanotechnology 23:135603. doi:10.1088/0957-4484/23/13/135603

Simakin AV, Voronov VV, Shafeev GA, Brayner R, Bozon-Verduraz F (2001) Nanodisks of Au and Ag produced by laser ablation in liquid environment. Chem Phys Lett 348:182–186. doi:10.1016/S0009-2614(01)01136-8

Sonay AY, Çağlayan AB, Çulha M (2012) Synthesis of peptide mediated Au core-Ag shell nanoparticles as surface-enhanced Raman scattering labels. Plasmonics 7:77–86. doi:10.1007/s11468-011-9278-4

Sylvestre J-P, Kabashin AV, Sacher E, Meunier M, Luong JHT (2004) J Am Chem Soc 126:7176–7177. doi:10.1021/ja048678s